PROCEEDINGS A

royalsocietypublishing.org/journal/rspa

Research

Cite this article: Martins Afonso M, Mitra D, Vincenzi D. 2019 Kazantsev dynamo in turbulent compressible flows. *Proc. R. Soc. A* **475**: 20180591.
http://dx.doi.org/10.1098/rspa.2018.0591

Received: 31 August 2018
Accepted: 25 January 2019

Subject Areas:
astrophysics, fluid mechanics

Keywords:
dynamo theory, compressible turbulence, Kazantsev model

Author for correspondence:
Dario Vincenzi
e-mail: dario.vincenzi@unice.fr

Kazantsev dynamo in turbulent compressible flows

Marco Martins Afonso[1], Dhrubaditya Mitra[2] and Dario Vincenzi[3]

[1]Centro de Matemática (Faculdade de Ciências) da Universidade do Porto, Rua do Campo Alegre 687, Porto 4169-007, Portugal
[2]Nordita, KTH Royal Institute of Technology and Stockholm University, Stockholm, Sweden
[3]Université Côte d'Azur, CNRS, LJAD, Nice 06100, France

DV, 0000-0003-3332-3802

We consider the kinematic fluctuation dynamo problem in a flow that is random, white-in-time, with both solenoidal and potential components. This model is a generalization of the well-studied Kazantsev model. If both the solenoidal and potential parts have the same scaling exponent, then, as the compressibility of the flow increases, the growth rate decreases but remains positive. If the scaling exponents for the solenoidal and potential parts differ, in particular if they correspond to typical Kolmogorov and Burgers values, we again find that an increase in compressibility slows down the growth rate but does not turn it off. The slow down is, however, weaker and the critical magnetic Reynolds number is lower than when both the solenoidal and potential components display the Kolmogorov scaling. Intriguingly, we find that there exist cases, when the potential part is smoother than the solenoidal part, for which an increase in compressibility increases the growth rate. We also find that the critical value of the scaling exponent above which a dynamo is seen is unity irrespective of the compressibility. Finally, we realize that the dimension $d = 3$ is special, as for all other values of d the critical exponent is higher and depends on the compressibility.

1. Introduction

Astrophysical objects typically have magnetic fields over many ranges of scales. The growth and saturation of these magnetic fields are the subject of dynamo theory. Most astrophysical flows are turbulent, hence the

THE ROYAL SOCIETY PUBLISHING

astrophysically relevant magnetic fields are generated by turbulent dynamos. Broadly speaking, we understand two different kinds of dynamo mechanism in turbulent fluids [1]: (a) one that generates magnetic fields whose characteristic length scales are significantly larger than the energy-containing length scales of the flow—large-scale dynamos; and (b) one that generates small-scale magnetic fields—the fluctuation dynamo. The small-scale tangled magnetic fields in the interstellar medium (ISM) or the Sun are supposed to be generated by the fluctuation dynamo. If we are interested in only the initial growth of the magnetic field but not its saturation, then we can ignore the Lorentz force by which the magnetic field acts back on the flow and reduce a nonlinear problem to a linear one—the kinematic dynamo problem. A pioneering work on the kinematic fluctuation dynamo was by Kazantsev [2], who approximated the velocity field by a random function of space and time. In particular, the velocity field is assumed to be statistically stationary, homogeneous and isotropic with zero divergence (under the latter assumption the velocity is called solenoidal or incompressible). It is also assumed to be short-correlated in time, more specifically white-in-time, and its correlation function in space is assumed to have a power-law behaviour with an exponent $0 \leq \xi \leq 2$. By virtue of the white-in-time nature of the velocity field, it is possible to write down a closed equation for the equal-time two-point correlation function of the magnetic field. Consequently, it is possible to show that a dynamo exists—the magnetic energy grows exponentially in time—iff the exponent $\xi > 1$ [3]. This result is an example of an anti-dynamo theorem. The Kazantsev model has played an important role in our understanding of the kinematic fluctuation dynamo excited by turbulent flows *à la* Kolmogorov, see e.g. the review by Brandenburg & Subramanian [1] and references therein. The same model for the velocity field has been extensively used to study the scaling behaviour and intermittency of advected passive scalar fields—the Kraichnan model [4] of passive-scalar turbulence, see e.g. [5] for a review.

In this paper, we are interested in a generalization of the Kazantsev model to *compressible* turbulence, which is relevant for the fluctuation dynamo in the ISM [6–8]. To the best of our knowledge, the earliest attempt to generalize the Kazantsev model to compressible flows was by Kazantsev *et al.* [9], who modelled the flow not by a white-in-time process but by random weakly damped sound waves, with energy concentrated on a single wavenumber, to find that the growth rate of the dynamo is proportional to the fourth power of the Mach number. More recently, Rogachevskii & Kleeorin [10] generalized the Kazantsev model to compressible flows, preserving its white-in-time nature, but adding a potential (irrotational) component to the velocity field. Both the solenoidal and the potential components are assumed to have the same scaling exponent, $0 \leq \xi \leq 2$. In this model, Rogachevskii & Kleeorin [10] found that the inclusion of compressible modes always makes it more difficult to excite the dynamo. Later Schekochihin & Kulsrud [11] and Schekochihin *et al.* [12] studied the same problem for the case of smooth velocity fields, $\xi = 2$, which corresponds to the limit of large magnetic Prandtl numbers. For understanding the magnetic-field growth in ISM, Schober *et al.* [13] incorporated compressibility into a generalization of the Kazantsev model previously proposed by Subramanian [14]. However, a tensor function can be the correlation of an isotropic vector field iff the corresponding longitudinal and normal three-dimensional spectra are non-negative [15, p. 41]: the velocity correlation prescribed by Subramanian [14] and then by Schober *et al.* [13] does not satisfy such condition. In addition, in the model of Schober *et al.* [13] the scaling exponent of the velocity correlation and the degree of compressibility are not independent parameters. In particular, for the Kolmogorov scaling the velocity is incompressible; this limit of the Kazantsev model has been studied in many papers before. The focus of our study is, in contrast, on the dependence of the dynamo effect upon the degree of compressibility.

Recent direct numerical simulations of compressible fluid turbulence [16–19] have shown that the spectra of the flow can be separated into a solenoidal and a potential part, where the solenoidal part scales with an exponent quite close to the classical Kolmogorov result for incompressible turbulence—the energy spectrum of the solenoidal part scales with an exponent of $-5/3$ in the inertial range—and the scaling exponent for the potential part is close to that of the turbulent Burgers equation—the energy spectrum of the potential part scales with an exponent of -2 in

the inertial range. How will the Kazantsev dynamo problem change if we use two independent scaling exponents for the solenoidal and the potential parts of the energy spectrum of the velocity field? This is the main task we set for ourselves in this paper.

We end this introduction by a warning to our reader: because of the popularity of the Kazantsev model as an analytically tractable model for the turbulent dynamo, the literature on it is large and diverse. We have so far cited only those papers that are directly relevant to our work. For a detailed introduction, we suggest several reviews [1,5,20,21] and references therein.

2. Model

We model the plasma as a conducting fluid at scales where the magnetohydrodynamics (MHD) equations are valid. Consequently, the magnetic field, $\boldsymbol{B}(\boldsymbol{x},t)$, evolves according to the induction equation [22]

$$\partial_t \boldsymbol{B} = \boldsymbol{\nabla} \times (\boldsymbol{u} \times \boldsymbol{B} - \kappa \boldsymbol{J}), \tag{2.1}$$

where $\boldsymbol{J} = \boldsymbol{\nabla} \times \boldsymbol{B}$ is the current, κ the magnetic diffusivity and $\boldsymbol{u}(\boldsymbol{x},t)$ the velocity. Furthermore, Maxwell's equations imply $\boldsymbol{\nabla} \cdot \boldsymbol{B} = 0$. Two dimensionless numbers characterize the MHD equations: the Reynolds number $Re \equiv VL/\nu$ and the magnetic Reynolds number $Re_\mathrm{m} \equiv VL/\kappa$, where V is a typical large-scale velocity, L is the correlation length of the velocity field and ν the kinematic viscosity of the fluid. The ratio of Re_m and Re is the magnetic Prandtl number $Pr \equiv \nu/\kappa$.

Instead of solving the momentum equation for the velocity, as is usual in MHD, the Kazantsev model assumes that the velocity $\boldsymbol{u}$ is a statistically stationary, homogeneous, isotropic and parity invariant, Gaussian random field. The statistics of a Gaussian field is entirely defined by its mean and second-order correlation. In the Kazantsev model, the mean of $\boldsymbol{u}$ is zero and the correlation is

$$\langle u_i(\boldsymbol{x}+\boldsymbol{r},t) u_j(\boldsymbol{x},t')\rangle = \mathscr{D}_{ij}(\boldsymbol{r})\delta(t-t'), \quad i,j=1,\ldots,d, \tag{2.2}$$

where d is the spatial dimension of the flow. In this paper, we use $d=3$ except in §4, where results for general d are presented. The velocity field is also assumed to be Galilean invariant, hence it is useful to introduce the second-order structure function $S_{ij}(\boldsymbol{r}) = \mathscr{D}_{ij}(0) - \mathscr{D}_{ij}(\boldsymbol{r})$, which is a Galilean invariant quantity that describes the statistics of the velocity increments. In view of statistical isotropy and parity invariance, $S_{ij}(\boldsymbol{r})$ takes the form[1] [15,23]

$$S_{ij}(\boldsymbol{r}) = S_\mathrm{N}(r)\delta_{ij} + [S_\mathrm{L}(r) - S_\mathrm{N}(r)]\hat{r}_i\hat{r}_j, \tag{2.3}$$

where $\hat{r}_i = r_i/r$ and $S_\mathrm{N}(r)$ and $S_\mathrm{L}(r)$ are called the normal (also known as transverse or lateral) and longitudinal second-order structure functions, respectively.

(a) Solenoidal random flows

Kazantsev [2] considered the three-dimensional solenoidal case ($\nabla \cdot \boldsymbol{u} = 0$) and the limits of vanishing Pr and infinite Re and Re_m, in which the velocity structure functions are scale invariant:

$$S_\mathrm{L}(r) = 2Dr^\xi \quad \text{and} \quad S_\mathrm{N}(r) = (\xi+2)Dr^\xi. \tag{2.4}$$

The positive constant D determines the magnitude of the fluctuations of the velocity increments, while the scaling exponent ξ varies between 0 and 2, the latter value describing a spatially smooth velocity field. For the above choice of the structure functions, the spectrum of the velocity $\boldsymbol{u}$ takes the form $E(k) \propto k^{-1-\xi}$.

We remind the reader that, owing to the δ-correlation in time, some care should be taken in comparing the velocity field $\boldsymbol{u}$, defined in (2.2), with a turbulent flow. Indeed, the eddy diffusivity of a three-dimensional turbulent flow scales as $r^{4/3}$, which yields Richardson's Law for the separation $R(t)$ between two fluid particles: $\langle R^2(t)\rangle \sim t^3$ [24]. In the δ-correlated field $\boldsymbol{u}$, the eddy diffusivity scales as r^ξ and fluid particles separate according to the following law: $\langle R^2(t)\rangle \sim t^{2/(2-\xi)}$ [5]. Therefore, in order for the δ-correlated velocity field to reproduce Richardson's Law, the

[1]Note that our definitions of the structure functions differ from those of Monin & Yaglom [15] by a factor of 2.

scaling exponent ξ must be taken equal to 4/3. Analogously, if the structure functions of a time-correlated three-dimensional incompressible flow scale as r^α (or equivalently its spectrum scales as $k^{-1-\alpha}$) the eddy diffusivity of such a flow behaves as $r^{1+\alpha/2}$ and the associated law of fluid-particle dispersion is $\langle R^2(t)\rangle \sim t^{4/(2-\alpha)}$. In this case, the time-correlated flow and the δ-correlated one yield the same scaling for the eddy diffusivity, and hence the same law of Lagrangian dispersion, if $\xi = 1 + \alpha/2$ [5, pp. 926–927].

(b) Compressible random flows

One way to include the effect of compressibility into the Kazantsev model is to modify, in d-dimensions, $S_\mathrm{L}(r)$ and $S_\mathrm{N}(r)$ as follows [25–27]:

$$S_\mathrm{L}(r) = Dr^\xi(d-1)(\wp\xi+1) \quad \text{and} \quad S_\mathrm{N}(r) = Dr^\xi(-\wp\xi+\xi+d-1), \tag{2.5}$$

by introducing a new parameter $\wp$ which is the degree of compressibility of the velocity field and varies between 0 (solenoidal, or incompressible, flow) and 1 (potential, or irrotational, flow). In this model, both the solenoidal and the potential parts of the flow have the same scaling exponent.

Two regimes can be identified depending on the value of $\wp$ [27]. In the regime of weak compressibility ($\wp < d/\xi^2$), fluid particles still separate according to the law $\langle R^2(t)\rangle \sim t^{2/(2-\xi)}$. Hence the same argument as for the incompressible case can be repeated to connect ξ and the scaling exponent α of the structure functions of a time-correlated flow, which yields $\xi = 1 + \alpha/2$. For instance, if a three-dimensional time-correlated flow displays the Burgers scaling ($\alpha = 1$), then the same law of Lagrangian dispersion is obtained in the δ-correlated velocity field if $\xi = 3/2$.

In the regime of strong compressibility ($\wp \geq d/\xi^2$), by contrast, the low powers of the particle separation decay in time, while the high ones grow but more slowly than in the weakly compressible case. The reason for this behaviour is the collapse of Lagrangian trajectories due to compressibility effects. Therefore, the dimensional argument used above to connect ξ and α does not hold in the regime of strong compressiblity. Moreover, this latter regime can only be observed for $d \leq 4$, as $\wp \leq 1$.

3. Results

(a) Closed equation for the correlation function of the magnetic field

Given the velocity field the task is to calculate the equations obeyed by the correlation functions of the magnetic field, where the averages are calculated over the statistics of the velocity field. The magnetic field is assumed to have the same spatial statistical symmetries as the velocity field. Its correlations are thus written as

$$C_{ij}(\boldsymbol{r},t) = C_\mathrm{L}(r,t)\delta_{ij} + \frac{r}{d-1}\partial_r C_\mathrm{L}(r,t)(\delta_{ij} - \hat{r}_i\hat{r}_j), \tag{3.1}$$

where a single scalar function $C_\mathrm{L}(r,t)$ is sufficient to define $C_{ij}(\boldsymbol{r},t)$ thanks to the solenoidality of the magnetic field [15,23].

By virtue of the Gaussian and white-in-time nature of the velocity field, it is possible to write a closed equation for the evolution of $C_{ij}(\boldsymbol{r},t)$ in a straightforward manner, by using the induction equation (2.1) and then averaging over the statistics of the velocity field. To obtain a closed equation, however, we need to calculate averages of a triple product: that of the velocity field, of the magnetic field and of its spatial derivative. This has been obtained by many different methods. A well-established approach employs a result known as 'Gaussian integration by parts': for a Gaussian, not-necessarily white-in-time, vector-valued noise $\boldsymbol{z}(t)$, with components $z_j(t)$, and its arbitrary functional $F(\boldsymbol{z})$,

$$\langle F(\boldsymbol{z})z_j(t)\rangle = \int \mathrm{d}s\, \langle z_j(t)z_k(s)\rangle \left\langle \frac{\delta F}{\delta z_k(s)} \right\rangle, \tag{3.2}$$

see e.g. §4.2 in [28] for a proof. At the next step, we need to integrate (2.1) formally to obtain the magnetic field as a function of the velocity field and then to calculate the necessary functional

derivatives. Then we have to take the limit $s \to t$. As the noise correlation becomes singular in this limit, we need to replace the Dirac delta function by a regularized even function and then take the limits. This regularization is equivalent to using the Stratonovich prescription for the noise. This method has been used extensively in dynamo theory (see, e.g. [3,11,12,29,30]) to calculate similar or higher-order correlation functions. Hence, we skip the details of the derivation and directly write down the result (see also [12] and references therein):

$$\partial_t C_L = (2\kappa + S_L)\partial_r^2 C_L + \left[\frac{2(d+1)}{r}\kappa + \partial_r S_L + \frac{2(d-1)}{r}S_L + \frac{3-d}{r}S_N\right]\partial_r C_L + \frac{d-1}{r}\left[\partial_r S_L + \partial_r S_N + \frac{d-2}{r}(S_L - S_N)\right]C_L. \tag{3.3}$$

(b) Schrödinger formulation

One of Kazantsev's main results is the formulation of the turbulent dynamo effect as the trapping of a quantum particle in a one-dimensional potential whose shape is determined by the functional form of the velocity structure functions [2]. This formulation leads to an appealing interpretation of the dynamo effect.

Equation (3.3) is a partial differential equation with one space and one time dimension. By the substitution

$$C_L(r,t) = \psi(r,t) r^{-(d-1)}[2\kappa + S_L(r)]^{-1/2} \exp\left[\frac{d-3}{2}\int r^{-1}\frac{2\kappa + S_N(r)}{2\kappa + S_L(r)}\mathrm{d}r\right], \tag{3.4}$$

(3.3) is turned into an imaginary-time Schrödinger equation with space-dependent mass for the function $\psi(r,t)$ [12]:

$$m(r)\partial_t\psi = \partial_r^2\psi - m(r)U(r)\psi, \tag{3.5}$$

with

$$m(r) = \frac{1}{2\kappa + S_L(r)} \tag{3.6}$$

and

$$U(r) = \frac{\partial_r^2 S_L(r)}{2} - \frac{[\partial_r S_L(r)]^2}{4[2\kappa + S_L(r)]} + \frac{(d-3)^2[2\kappa + S_N(r)]^2}{4r^2[2\kappa + S_L(r)]} + \frac{(3d-5)[2\kappa + S_N(r) - r\partial_r S_N(r)]}{2r^2}. \tag{3.7}$$

The function $\psi(r,t)$ has the same time dependence as $C_L(r,t)$. We therefore seek solutions of the form $\psi(r,t) = \psi_\gamma(r)\,\mathrm{e}^{-\gamma t}$, where $\psi_\gamma(r)$ are the eigenstates of the Schrödinger operator in (3.5) and γ the associate energies. The magnetic correlation grows in time if there exist negative-energy ($\gamma < 0$) eigenstates. If so, the energy of the ground state, γ_0, yields the asymptotic growth rate $|\gamma_0|$.[2] From (3.5), γ can be written as follows:

$$\gamma = \frac{\int m(r)U(r)\psi_\gamma^2(r)\,\mathrm{d}r + \int[\psi_\gamma'(r)]^2\,\mathrm{d}r}{\int m(r)\psi_\gamma^2(r)\,\mathrm{d}r}. \tag{3.8}$$

As $m(r) > 0$ for all r [12], γ is negative iff the effective potential $U_{\mathrm{eff}}(r) \equiv m(r)U(r)$ admits negative energies. Thus the problem of the growth of the magnetic correlations is mapped into that of the existence of negative-energy states for the one-dimensional potential $U_{\mathrm{eff}}(r)$—the energy for the ground state of the potential $U_{\mathrm{eff}}(r)$ is equal to the growth rate of the fastest growing mode in the kinematic dynamo problem.

[2]Note that here the magnetic growth is studied at non-zero κ. As the $\kappa \to 0$ limit is singular [31], the asymptotic growth rate in a perfectly conducting fluid ($\kappa = 0$) cannot be deduced from the results described here by letting κ tend to zero.

(c) Solenoidal random flows

In the original Kazantsev model, the flow is assumed to be solenoidal and the longitudinal and normal structure functions have the same scaling exponent as given in (2.4). The effective potential is obtained by substituting $d=3$ and the expressions of S_L and S_N from (2.4) in (3.3), and simplifying (e.g. [3]):

$$U_{\text{eff}}(r) = \frac{8\kappa^2 - 2(\xi^2+3\xi-8)\kappa D r^\xi - (3\xi^2+6\xi-8)D^2 r^{2\xi}}{4r^2(\kappa + Dr^\xi)^2}$$
$$= \frac{8r_\kappa^{2\xi} - 2(\xi^2+3\xi-8)r_\kappa^\xi r^\xi - (3\xi^2+6\xi-8)r^{2\xi}}{4r^2(r_\kappa^\xi + r^\xi)^2}, \tag{3.9}$$

where in the second step, we have introduced the diffusive scale, $r_\kappa \equiv (\kappa/D)^{1/\xi}$, at which the diffusive and the advective terms in the induction equation (2.1) balance each other. For $r \ll r_\kappa$, $U_{\text{eff}}(r) \sim 2/r^2$ and is therefore repulsive. For $r \gg r_\kappa$, $U_{\text{eff}}(r) \sim -(3\xi^2/4 + 3\xi/2 - 2)/r^2$; hence the effective potential is negative at large r. By examining the shape of $U_{\text{eff}}(r)$, it is possible to conclude that the critical value of ξ for the kinematic dynamo effect is $\xi_{\text{crit}} = 1$ [2] (see also [3]). For $\xi < 1$, $U_{\text{eff}}(r)$ is indeed everywhere greater than a potential of the form $-c/r^2$ with $c < 1/4$, which does not have any negative-energy eigenstates [32]. Hence the same holds for $U_{\text{eff}}(r)$, and consequently no dynamo exists. For $\xi > 1$, the effective potential behaves at large distances as $U_{\text{eff}}(r) \sim -c/r^2$ with $c > 1/4$. A potential with such a large-r behaviour has a discrete spectrum containing an infinite number of negative-energy levels [32], so the magnetic correlation can grow exponentially.

For a smooth flow ($\xi = 2$), the value of the growth rate is known analytically: $|\gamma_0| = 15D/2$ [2,31,33], and the magnetic correlation decays as $C_L(r) \sim r^{-5/2}$ [31]. For a spatially rough flow, $1 < \xi < 2$, the analytical calculation of $|\gamma_0|$ is a difficult task. It was obtained numerically in [2] and [34], and an analytical estimate was given by Arponen & Horvai [35]. The growth rate increases as a function of ξ, i.e. a greater degree of spatial regularity of the velocity field favours the magnetic growth. In addition, the magnetic correlation decays as a stretched exponential of the spatial separation with stretching exponent $1 - \xi/2$ [34].

The incompressible case was generalized to d dimensions by Gruzinov *et al.* [33] and Vergassola [3]. In particular, for $d = 2$, $U_{\text{eff}}(r)$ is repulsive everywhere and hence there cannot be dynamo effect, in accordance with Zel'dovich's anti-dynamo theorem [36].

(d) Compressible random flows

Next we consider the model of compressible flow given by (2.5), where both the solenoidal and the potential components of the structure functions scale with the same exponent. Upon substitution of (2.5) into (3.6) and (3.7), the mass and potential functions are found to have the form

$$m(r) = \frac{1}{2\kappa + Dr^\xi(d-1)(\wp\xi+1)} \tag{3.10}$$

and

$$U(r) = \frac{a_0 + a_1 r^\xi + a_2 r^{2\xi}}{4r^2[2\kappa + Dr^\xi(d-1)(\wp\xi+1)]}, \tag{3.11}$$

where the coefficients a_0, a_1, a_2 are given in appendix A.

Let us examine the $d = 3$ case. At small distances ($r \ll r_\kappa$), the asymptotic behaviour of $U_{\text{eff}}(r)$ is unchanged compared to the incompressible case. For $r \gg r_\kappa$,

$$U_{\text{eff}}(r) \sim \frac{\wp\xi^3 + 2\wp\xi^2 - 3\xi^2 - 4\wp\xi - 6\xi + 8}{4(\wp\xi+1)r^2}. \tag{3.12}$$

By studying the form of $U_{\text{eff}}(r)$ as in §3c, it can be shown that the critical value of ξ for the dynamo effect is not affected by the degree of compressibility, i.e. $\xi_{\text{crit}} = 1$ for all values of $\wp$ [10]. Indeed, for $\xi < 1$, $U_{\text{eff}}(r)$ behaves asymptotically as $-c/r^2$ with $c < 1/4$, and both a_0 and a_1 are positive

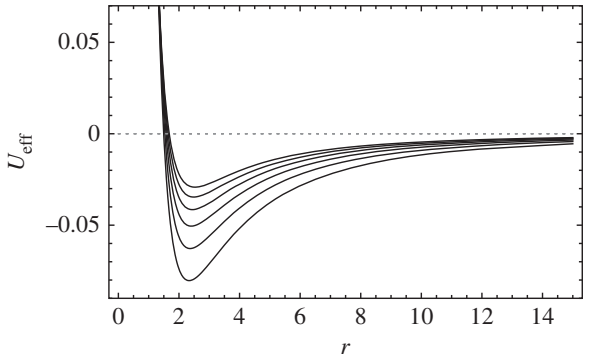

Figure 1. Effective potential for $\xi = 4/3$ and, from bottom to top, $\wp = 0, 0.2, 0.4, 0.6, 0.8, 1$.

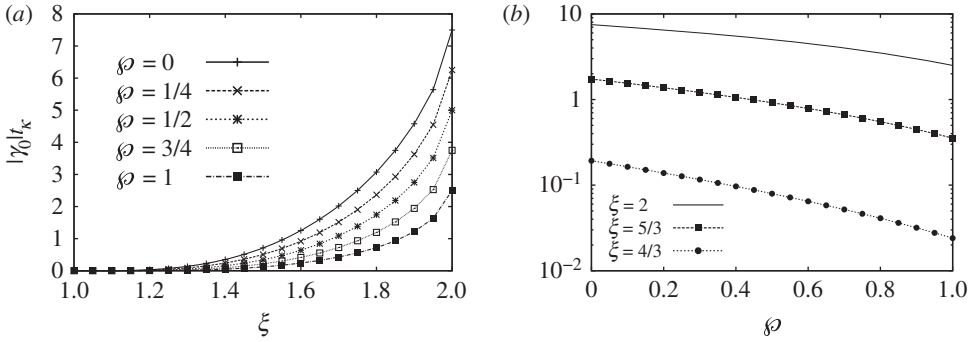

Figure 2. Magnetic growth rate multiplied by the diffusive time as a function of: (*a*) the scaling exponent ξ of the velocity structure functions and (*b*) the degree of compressibility $\wp$ of the flow. The solid line in the right panel shows the analytical expression for $\xi = 2$ [12].

for all values of $\wp$. Hence $U_{\rm eff}(r) > -c/r^2$ with $c < 1/4$ for all r, and it does not admit negative-energy eigenstates. For $\xi > 1$, $U_{\rm eff}(r) \sim -c/r^2$ with $c > 1/4$, and an infinite number of states with negative energy can exist. Figure 1 shows the effect of compressibility on the shape of the effective potential.

Even though $\xi_{\rm crit}$ does not vary with $\wp$, for $\xi > 1$ the magnetic growth is affected by the degree of compressibility of the flow. For $\xi = 2$, the growth rate is $|\gamma_0| = (15/2 - 5\wp)D$, while at large separations and long times the correlation $C_{\rm L}(r, t)$ behaves, up to logarithmic corrections, as $r^{-5/2}\exp(|\gamma_0|t)$ [12].

For $1 < \xi < 2$, to the best of our knowledge, no analytical expression for the growth rate $|\gamma_0|$ is available. We calculate it numerically by applying to (3.5) a variation–iteration method that is similar to techniques used to find the largest eigenvalue of very large matrices. This method is described in detail in appendix B. The result is shown in figure 2, where we plot $|\gamma_0|t_\kappa$ versus ξ for several values of $\wp$; here $t_\kappa \equiv r_\kappa^2/\kappa$ is the time scale associated with magnetic diffusion. We find that, irrespective of $\wp$, the growth rate is positive for all values of $\xi > 1$ and increases with ξ, i.e. as the spatial regularity of the flow improves. Note that, for $\wp = 1$, the values of ξ such that $\xi > \sqrt{3}$ are in the strongly compressible regime (see §2). For a fixed ξ, the effect of compressibility is always to decrease the growth rate, i.e. to make the dynamo weaker. Rogachevskii & Kleeorin [10] tried to estimate the growth rate by asymptotic matching; they also found the same qualitative effect of compressibility.

We find out the behaviour of $C_{\mathrm{L}}(r,t)$ for large r by replacing $m(r)$ and $U(r)$ in (3.5) with their asymptotic expressions. The resulting equation for $\psi_\gamma(r)$ is a Bessel differential equation, whose non-diverging solution is

$$\psi_\gamma(r) \propto \sqrt{r} K_b\left[\beta\sqrt{\frac{|\gamma|}{D}} r^{1-\xi/2}\right] = \sqrt{r}\, K_b\left[\beta\sqrt{|\gamma|t_\kappa}\left(\frac{r}{r_\kappa}\right)^{1-\xi/2}\right], \tag{3.13}$$

where $\beta = b\sqrt{2/(\wp\xi+1)}$ and K_b is the modified Bessel function of the second kind of order $b = 1/(2-\xi)$. At large r this solution behaves as $\exp[-\beta\sqrt{|\gamma|t_\kappa}(r/r_\kappa)^{1-\xi/2}]$. Furthermore, the long-time behaviour of the magnetic correlation is determined by the ground state $\psi_{\gamma_0}(r)$. From (3.4) we therefore conclude that, for $r \gg r_\kappa$ and $t \gg t_\kappa$,

$$C_{\mathrm{L}}(r,t) \propto r^{-2-\xi/2} \exp\left[-\beta\sqrt{|\gamma_0|t_\kappa}\left(\frac{r}{r_\kappa}\right)^{1-\xi/2}\right] \mathrm{e}^{|\gamma_0|t}. \tag{3.14}$$

As far as the spatial dependence of the magnetic correlation is concerned, we thus recover the stretched-exponential behaviour of the incompressible case; the degree of compressibility of the flow only affects $|\gamma_0|$, and hence the rate at which the stretched exponential function decays in space, but not the stretching exponent.

(e) Solenoidal–potential decomposition

The results of the previous section indicate that the spatial regularity of the flow favours the magnetic growth, whereas compressibility hinders it. It has now been realized that for turbulence at moderate Mach numbers the solenoidal and potential parts of the flow have different scaling exponents; more precisely, the solenoidal part of the velocity spectrum displays the Kolmogorov scaling $k^{-5/3}$, while the potential one displays the Burgers scaling k^{-2} [16–19]. It is therefore interesting to investigate the interplay between spatial regularity and compressibility in the case where the potential part of the flow is more regular than the solenoidal one. We thus consider the following velocity structure functions (see [15], p. 57, for the solenoidal–potential decomposition of an isotropic random field):

$$S_{\mathrm{L}}(r) = 2(1-\wp)D_{\mathrm{S}} r^{\xi_{\mathrm{S}}} + 2\wp D_{\mathrm{P}}(1+\xi_{\mathrm{P}}) r^{\xi_{\mathrm{P}}} \tag{3.15}$$

and

$$S_{\mathrm{N}}(r) = (1-\wp)D_{\mathrm{S}}(2+\xi_{\mathrm{S}}) r^{\xi_{\mathrm{S}}} + 2\wp D_{\mathrm{P}} r^{\xi_{\mathrm{P}}}, \tag{3.16}$$

where ξ_{S} and ξ_{P} are the scaling exponents of the solenoidal ($\wp = 0$) and potential ($\wp = 1$) components, respectively, and D_{P} and D_{S} are positive coefficients. Varying the degree of compressibility thus interpolates linearly between a solenoidal flow with scaling exponent ξ_{S} and a potential flow with exponent ξ_{P}.

The mass and the potential functions can be calculated by inserting $S_{\mathrm{L}}(r)$ and $S_{\mathrm{N}}(r)$ from (3.15) and (3.16) into (3.6) and (3.7):

$$m(r) = \frac{1}{2[\kappa + (1-\wp)D_{\mathrm{S}} r^{\xi_{\mathrm{S}}} + \wp D_{\mathrm{P}} r^{\xi_{\mathrm{P}}}]} \tag{3.17}$$

and

$$\begin{aligned} U(r) = &-\frac{[(1-\wp)\xi_{\mathrm{S}} D_{\mathrm{S}} r^{-1+\xi_{\mathrm{S}}} + \wp\xi_{\mathrm{P}}(1+\xi_{\mathrm{P}}) D_{\mathrm{P}} r^{-1+\xi_{\mathrm{P}}}]^2}{2[\kappa + (1-\wp)D_{\mathrm{S}} r^{\xi_{\mathrm{S}}} + \wp(1+\xi_{\mathrm{P}}) D_{\mathrm{P}} r^{\xi_{\mathrm{P}}}]} \\ &+ \frac{4\kappa}{r^2} + (1-\wp)(1-\xi_{\mathrm{S}})(4+\xi_{\mathrm{S}}) D_{\mathrm{S}} r^{-2+\xi_{\mathrm{S}}} + \wp(4-5\xi_{\mathrm{P}}+\xi_{\mathrm{P}}^3) D_{\mathrm{P}} r^{-2+\xi_{\mathrm{P}}}. \end{aligned} \tag{3.18}$$

The product of $m(r)$ and $U(r)$ yields the effective potential. In the diffusive range, $r \ll r_\kappa$, $U_{\mathrm{eff}}(r) \sim 2/r^2$ independently of the values of ξ_{S} and ξ_{P}; the dynamics is indeed dominated by magnetic diffusion in this range. If $\xi_{\mathrm{S}} > \xi_{\mathrm{P}}$ ($\xi_{\mathrm{S}} < \xi_{\mathrm{P}}$), the asymptotic behaviour of $U_{\mathrm{eff}}(r)$ is the same as that of a solenoidal flow with exponent ξ_{S} (a potential flow with an exponent ξ_{P}). As noted in §3d, the critical value of the scaling exponent equals unity, $\xi_{\mathrm{crit}} = 1$, in both cases. Therefore, the critical

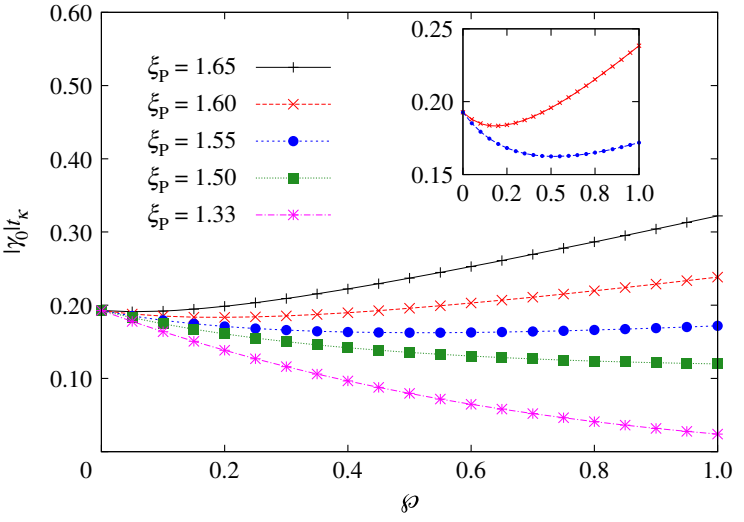

Figure 3. Magnetic growth rate multiplied by the diffusive time as a function of the degree of compressibility of the velocity field for $\xi_S = 4/3$ and different values of ξ_P. The $\xi_P = 1.55$ and $\xi_P = 1.60$ curves are plotted again in the inset, so that their non-monotonic behaviour is more easily appreciated. (Online version in colour.)

scaling exponent for the dynamo effect does not depend on whether or not the solenoidal and potential components scale differently, and if at least one of the two exponents is greater than unity, a dynamo is obtained.

The magnetic growth rate, by contrast, is expected to vary with the spatial regularity of the potential component. As for a generic $\wp$ the solenoidal and potential components of the velocity field now scale differently, two scales, $r_\kappa^{(S)} \equiv (\kappa/D_S)^{1/\xi_S}$ and $r_\kappa^{(P)} \equiv (\kappa/D_P)^{1/\xi_P}$, can be formed by balancing the diffusion term in (2.1) with either the solenoidal or the potential contribution to the advection term. In the calculation of the magnetic growth rate, we set $r_\kappa^{(S)} = r_\kappa^{(P)}$. The relative weight of the solenoidal and the potential components is thus determined solely by $\wp$. Furthermore, such choice allows us to define a single diffusive time scale t_κ, which is used to rescale the growth rate. We do not know any analytical method allowing us to exactly calculate the growth rate as a function of ξ and $\wp$. Hence we use the variation–iteration method to calculate it numerically. In figure 3, we plot the non-dimensionalized growth rate as a function of $\wp$ for $\xi_S = 4/3$ and for several different values of ξ_P. According to the discussion at the end of §2a, a turbulent velocity field with spectrum scaling as in [16–19], i.e. $k^{-5/3}$ for the solenoidal component and k^{-2} for the potential one, corresponds to a white-in-time flow with $\xi_S = 4/3$ and $\xi_P = 3/2$ (green square symbols in figure 3). The values $\xi_S = \xi_P = 4/3$ correspond to the case where both the solenoidal and the potential components of the white-in-time flow scale with Kolmogorov exponent (red $*$ symbols in figure 3). In both of these cases, the growth rate monotonically decreases as a function of $\wp$. But the growth rate for the case $\xi_S = 4/3$ and $\xi_P = 3/2$ is higher for all values of $\wp$. Remarkably, for greater values of ξ_P, we find that $|\gamma_0|$ *varies non-monotonically or even increases with* $\wp$ (inset of figure 3). Hence compressibility can increase the magnetic growth if the potential component of the flow is sufficiently regular. This is a new qualitative result.

(f) Critical magnetic Reynolds number

The magnetic Reynolds number Re_m measures the relative intensity of the stretching of magnetic lines by the flow and ohmic dissipation. Therefore, for the dynamo effect to take place, Re_m must be sufficiently high and exceed a critical value Re_m^{crit}.

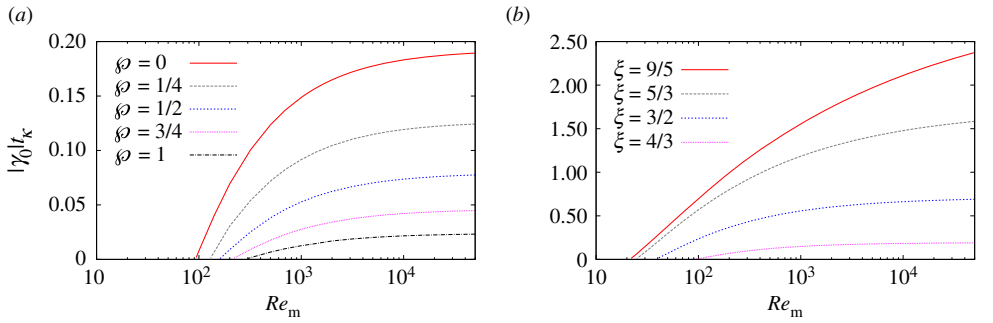

Figure 4. Magnetic growth rate multiplied by the diffusive time as a function of the magnetic Reynolds number for (*a*) $\xi = 4/3$ and from top to bottom $\wp = 0, 1/4, 1/2, 3/4, 1$ and (*b*) $\wp = 0$ and from top to bottom $\xi = 9/5, 5/3, 3/2, 4/3$. (Online version in colour.)

We consider first the case in which both the solenoidal and the potential components of the velocity field display the same scaling exponent ($\xi_S = \xi_P = \xi$). In the original version of the Kazantsev model, Re_m is infinite, as the structure functions of the velocity field are assumed to increase indefinitely with the scale separation. It is possible, however, to modify the form of $S_L(r)$ and $S_N(r)$ in such a way as to introduce a finite correlation length L beyond which the structure functions saturate to a constant value [12,37–41]. This allows the definition of the magnetic Reynolds number as $Re_m \equiv L/r_\kappa = L(D/\kappa)^{1/\xi}$. Here we follow [15, p. 55] (see also [5,34,35]) and introduce L in the model by modifying the velocity spectrum as follows:

$$E(k) \propto \frac{k^4}{(k^2 + L^{-2})^{(5+\xi)/2}} \tag{3.19}$$

(the reader is referred to appendix C for more details). The specific form of $E(k)$ is immaterial and only affects numerical details. What is important is that the power-law behaviour $E(k) \sim k^{-1-\xi}$ is recovered for $k \gg L^{-1}$, while $E(k)$ is regular for $k \ll L^{-1}$. The structure functions for finite Re_m can then be calculated from $E(k)$ (see appendix C) and can be inserted into (3.6) and (3.7) to obtain the effective potential $U_{eff}(r)$, and hence the magnetic growth rate via the variation–iteration method.

Within the Schrödinger formulation of the Kazantsev model, the existence of a critical magnetic Reynolds number can be interpreted thus: a finite value of L generates a potential barrier at spatial scales of the order of L and greater than it [12,34,38]. As L (and hence Re_m) is decreased, the potential well raises, until negative-energy states cease to exist and the dynamo disappears.

Figure 4 shows the rescaled magnetic growth rate as a function of Re_m (a) for fixed $\xi = 4/3$ and different values of $\wp$ and (b) for fixed $\wp = 0$ and different values of ξ. We find yet another instance in which the degree of compressibility and the spatial regularity of the flow have an opposite effect on the dynamo effect: compressibility increases Re_m^{crit}, whereas the smoothness of the flow makes it decrease.

It is thus interesting to examine the interplay between these two effects by considering, as in §3e, a velocity spectrum such that the solenoidal component of the velocity field displays the Kolmogorov scaling, while the potential one the Burgers scaling:

$$E(k) = (1 - \wp)\frac{A_S}{L^{\xi_S}} \frac{k^4}{(k^2 + L^{-2})^{(5+\xi_S)/2}} + \wp \frac{A_P}{L^{\xi_P}} \frac{k^4}{(k^2 + L^{-2})^{(5+\xi_P)/2}}. \tag{3.20}$$

Here, A_S and A_P are positive coefficients. The structure functions that yield the above spectrum can be found in appendix C.

Once more, we calculate the magnetic growth rate numerically by using the variation–iteration method. The scales $r_\kappa^{(S)}$ and $r_\kappa^{(P)}$ are defined as in §3e with D_S and D_P given in (C 7) and (C 8). We again set the ratio $r_\kappa^{(S)}/r_\kappa^{(P)}$ to unity; the values of Re_m and t_κ are thus unaffected by whether $r_\kappa^{(S)}$

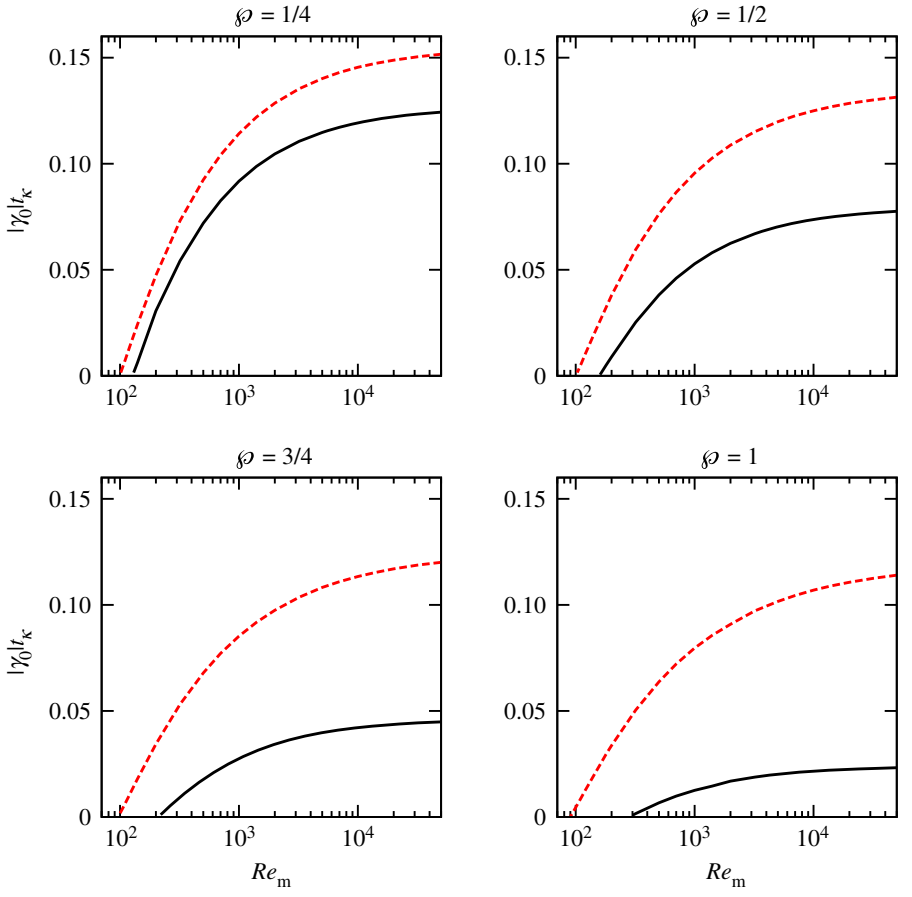

Figure 5. Magnetic growth rate multiplied by the diffusive time as a function of the magnetic Reynolds number for different values of $\wp$. The solid black curves correspond to $\xi_S = \xi_P = 4/3$; the dashed red ones to $\xi_S = 4/3$ and $\xi_P = 3/2$. (Online version in colour.)

or $r_\kappa^{(P)}$ is used in the definitions. The magnetic growth rate as a function of Re_m is shown in figure 5 for the case $\xi_S = 4/3$, $\xi_P = 3/2$ and for representative values of the degree of compressibility. Compared to the case $\xi_S = \xi_P = 4/3$, the critical magnetic Reynolds number is lower when the potential component of the flow displays the Burgers scaling. In this latter case, Re_m^{crit} depends weakly on $\wp$, which suggests that, for $\xi_P = 3/2$, the higher spatial regularity compensates the effect of the increase in compressibility. For higher values of ξ_P, the effect of the higher regularity of the potential component is expected to prevail and to make Re_m^{crit} decrease as a function of $\wp$.

4. Kinematic dynamo in *d* dimensions

In this section, we examine the dependence of the Kazantsev model (with single scaling exponent) on the space dimension. In (2.2), the dimension d may indeed be regarded as a parameter that can also take values different from 2 or 3. So far in this paper, we have limited ourselves to the case $d = 3$. Gruzinov *et al.* [33] showed that if the flow is smooth ($\xi = 2$) and incompressible ($\wp = 0$), there is dynamo effect only when the spatial dimension is in the interval $2.103 \leq d \leq 8.765$. Arponen & Horvai [35] extended this result to a rough flow ($0 < \xi < 2$) and showed that the curve ξ_{crit} versus d is convex and has its minimum in $d = 3$. Therefore, the range of spatial dimensions

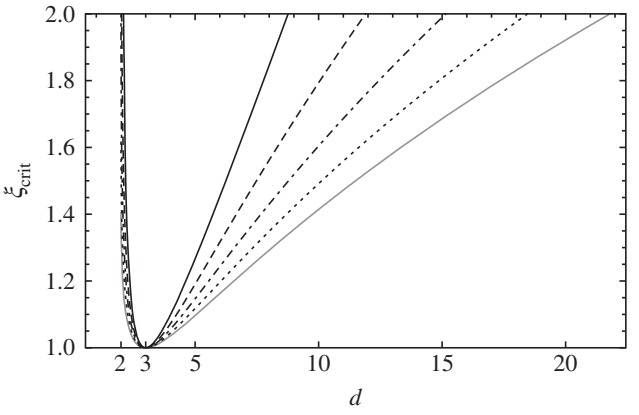

Figure 6. The critical scaling exponent for the dynamo effect versus the spatial dimension of the flow for different values of the degree of compressibility. From left to right: $\wp = 0$ (solid, black line), $\wp = 1/4$ (dashed line), $\wp = 1/2$ (dot-dashed line), $\wp = 3/4$ (dotted line), $\wp = 1$ (solid, grey line).

over which the dynamo effect can take place shrinks as the flow becomes rougher or, in other words, a higher degree of spatial regularity of the flow is necessary if $d \neq 3$.

To study the effect of compressibility on ξ_{crit} for a general dimension d, we once again examine the large-r form of $U_{eff}(r)$. By repeating the argument used in §§3c and 3d, we obtain that ξ_{crit} is the root of the following equation,

$$\frac{a_2}{4[D(d-1)(\wp\xi+1)]^2} = -\frac{1}{4}, \tag{4.1}$$

such that $0 \leq \xi_{crit} \leq 2$ (the coefficient a_2 is defined in (3.11) and (A 3)). Figure 6 shows ξ_{crit} as a function of d for different values of $\wp$. Clearly, the three-dimensional case is peculiar inasmuch as it is the only one for which ξ_{crit} does not depend upon $\wp$, and the critical exponent is the lowest for $d = 3$. For all other values of d, increasing $\wp$ broadens the range of spatial dimensions over which the magnetic correlation grows, and lowers the critical exponent for the appearance of the dynamo effect. No exponential growth of the magnetic field is found for $d = 2$ irrespective of the value of $\wp$.

5. Conclusion

In this paper, we have used a model that is a generalization of the Kazantsev model to flows that have both solenoidal and potential components. We find, in agreement with earlier results, that the critical value of the exponent above which a dynamo is seen is unity in all cases. If both the solenoidal and the potential parts have the same scaling exponent, then as the compressibility of the flow increases, the growth rate of the dynamo decreases but does not go to zero. In other words, even when the flow has only a potential component, the dynamo is not turned off but merely slowed down. This qualitative result was already known from the approximate analytical work of Rogachevskii & Kleeorin [10]; we have now provided numerical results that support the same conclusion. We also show that the flow compressibility increases the critical magnetic Reynolds number for the dynamo effect, whereas spatial regularity lowers it. More importantly, we have considered the more realistic case where the solenoidal and the potential parts have different scaling exponents. If we consider the case where these scaling exponents for the solenoidal and potential parts correspond to typical Kolmogorov and Burgers values, then we again reach the same qualitative conclusion—an increase in compressibility slows down the growth rate of the dynamo but does not turn it off. The slow down due to compressibility is,

however, weaker than in the case in which both the solenoidal and the potential components of the flow display a Kolmogorov scaling. Intriguingly, we find that there exist cases, if the potential part is significantly smoother than the solenoidal part, where an increase in compressibility can actually *increase* the dynamo growth rate. Unfortunately, this result remains a curiosity because we are not aware of any realistic flow that corresponds to such a case. If the potential component of the flow displays the Burgers scaling, we also show that the critical Reynolds number is lower than when both the solenoidal and the potential components display the Kolmogorov scaling. Finally, by considering the same model in general d dimensions, we realize that the dimension $d=3$ is special; for all other values of d, the critical value of the scaling exponent of the velocity structure functions depends on the degree of compressibility of the flow, in particular, increasing the compressibility lowers the critical value of the exponent.

The Kazantsev model is a rare example of a flow allowing an analytical study of the turbulent dynamo effect. For this reason, it has attracted a lot of attention in the literature, and several extensions of the model have been proposed to include certain properties of a turbulent velocity field that were not present in the original version. One should, of course, be careful in translating lessons learned from Kazantsev-type models to real astrophysical flows or to direct numerical simulations. These models are indeed limited by their white-in-time nature and their Gaussian statistics. Direct quantitative comparison between such models and simulations may therefore not be straightforward. Our results are furthermore limited by the fact that we consider a vanishing magnetic Prandtl number. We also note that here we have defined the dynamo effect in terms of the growth or decay of the volume average of the magnetic energy. In the usual stretch-twist-fold picture of Zeldovich, it is the magnetic flux that is considered. It has been shown in earlier works, see e.g. [29,31,42] , that the growth rate of different moments of the magnetic field can be different. Therefore, care should be taken in extending our results to moments of the magnetic field of an order different from the second. Nevertheless, the large literature on Kazantsev-type models shows that the qualitative insight gained from the study of such models is robust.

Data accessibility. This paper has no experimental data.

Authors' contributions. All the authors have contributed to the design of the study, derived the results and prepared the manuscript.

Competing interests. We have no competing interests.

Funding. M.M.A. was partially supported by CMUP (UID/MAT/00144/2013), funded by FCT (Portugal) with national (MEC) and European structural funds (FEDER), under the partnership agreement PT2020; and also by Project STRIDE - NORTE-01-0145-FEDER-000033, funded by ERDF NORTE 2020. D.M. is supported by grants from the Swedish Research Council (grant nos. 638-2013-9243 and 2016-05225).

Acknowledgements. The authors are grateful to Jérémie Bec, Axel Brandenburg, Antonio Celani, Igor Rogachevskii and Jennifer Schober for their useful suggestions.

Appendix A. Potential U for general d and $\wp$

For general d and $\wp$, the coefficients in the expression of the potential $U(r)$, see (3.11), are as follows:

$$a_0 = 4(d+1)(d-1)\kappa^2, \tag{A 1}$$

$$a_1 = 4D[2(\wp\xi^3 + \wp\xi^2 - \xi^2 + 2\wp\xi - 3\xi + 8) + (\wp\xi^3 + 2\wp\xi^2 - 2\xi^2 + 7\wp\xi - 8\xi + 20)(d-3) + 2(\wp\xi - \xi + 4)(d-3)^2 + (d-3)^3] \tag{A 2}$$

and

$$\begin{aligned} a_2 = D^2[&4(\wp^2\xi^4 + 2\wp^2\xi^3 - 2\wp\xi^3 - 4\wp^2\xi^2 - 4\wp\xi^2 - 3\xi^2 + 4\wp\xi - 6\xi + 8) \\ &+ 4(\wp^2\xi^4 + 3\wp^2\xi^3 - 3\wp\xi^3 - 5\wp^2\xi^2 - 8\wp\xi^2 - 4\xi^2 + 9\wp\xi - 11\xi + 14)(d-3) \\ &+ (\wp^2\xi^4 + 4\wp^2\xi^3 - 4\wp\xi^3 - 5\wp^2\xi^2 - 26\wp\xi^2 - 4\xi^2 + 22\wp\xi - 24\xi + 36)(d-3)^2 \\ &- 2(3\wp\xi^2 - 2\wp\xi + 2\xi - 5)(d-3)^3 + (d-3)^4]. \end{aligned} \tag{A 3}$$

Appendix B. Variation–iteration method

The variation–iteration technique proposed by Morse & Feshbach [43] represents a useful tool for calculating $\psi_{\gamma_0}(r)$ and $|\gamma_0|$. It was applied earlier to the study of the kinematic dynamo effect in the incompressible Kazantsev model [34] and is summarized below.

We first note that the eigenfunction $\psi_\gamma(r)$ satisfies the equation:

$$\frac{\mathrm{d}^2\psi_\gamma}{\mathrm{d}r^2} + m(r)[\gamma - U(r)]\psi_\gamma = 0. \tag{B 1}$$

The interval $[0,\infty)$ is then mapped into the bounded interval $(0,1]$ by means of the change of coordinate $\rho = (1+\mu)^{-r}$ with $\mu > 0$, which transforms (B 1) as follows:

$$\mathscr{L}\psi_\gamma = \lambda \mathscr{M}\psi_\gamma, \tag{B 2}$$

with

$$\mathscr{L} \equiv -[\ln(1+\mu)]^2 \frac{\mathrm{d}}{\mathrm{d}\rho}\left(\rho\frac{\mathrm{d}}{\mathrm{d}\rho}\right) + \frac{m(\rho)}{\rho}[U(\rho) - U_{\min}], \tag{B 3}$$

$\mathscr{M} \equiv m(\rho)/\rho$, and $\lambda \equiv \gamma - U_{\min}$. Here $U_{\min}$ denotes the minimum of the potential $U(\rho)$. The operators $\mathscr{L}$ and $\mathscr{M}$ are positive-definite and self-adjoint with respect to the usual inner product on $\mathrm{L}^2([0,1])$. In addition, for $\xi > 1$, the spectrum of eigenvalues λ is bounded from below and extends to infinity.

Let $\phi^{(0)}(\rho)$ be an initial trial function that is not orthogonal to $\psi_{\gamma_0}(\rho)$ and satisfies the boundary conditions $\phi^{(0)}(0) = \phi^{(0)}(1) = 0$. No other conditions are required for $\phi^{(0)}(\rho)$. The technique for calculating $\psi_{\gamma_0}(r)$ and $|\gamma_0|$ consists in iteratively applying the operator $\mathscr{L}^{-1}\mathscr{M}$, in such a way that the nth iterate $\phi^{(n)}(\rho)$ is given by

$$\phi^{(n)}(\rho) \equiv \mathscr{L}^{-1}\mathscr{M}\phi^{(n-1)}(\rho) = (\mathscr{L}^{-1}\mathscr{M})^n\phi^{(0)}(\rho) \tag{B 4}$$

and the corresponding eigenvalue estimate is

$$\lambda_0^{(n)} \equiv \frac{\int_0^1 \phi^{(n)}(\rho)\mathscr{L}\phi^{(n)}(\rho)\,\mathrm{d}\rho}{\int_0^1 \phi^{(n)}(\rho)\mathscr{M}\phi^{(n)}(\rho)\,\mathrm{d}\rho}. \tag{B 5}$$

As n is increased, $\phi^{(n)}(\rho)$ tends to $\psi_{\gamma_0}(\rho)$ and $\lambda_0^{(n)}$ to $\gamma_0 - U_{\min}$ (from above). The iteration is stopped once the desired convergence is obtained.

In numerical calculations, the interval $[0,1]$ is partitioned into N subintervals of size Δ and, for a generic function $f(\rho)$, the differential part of the operator $\mathscr{L}$ is discretized as follows:

$$\begin{aligned}\frac{\mathrm{d}}{\mathrm{d}\rho}\left(\rho\frac{\mathrm{d}f}{\mathrm{d}\rho}\right)\bigg|_{\rho_k} &= \frac{1}{2}\left(\frac{\rho_{k+1}f'_{k+1} - \rho_k f'_k}{\Delta} + \frac{\rho_k f'_k - \rho_{k-1}f'_{k-1}}{\Delta}\right)\\ &= \frac{1}{2\Delta}\left(\rho_{k+1}\frac{f_{k+1}-f_k}{\Delta} - \rho_k\frac{f_k - f_{k-1}}{\Delta} + \rho_k\frac{f_{k+1}-f_k}{\Delta} - \rho_{k-1}\frac{f_k - f_{k-1}}{\Delta}\right)\\ &= \frac{1}{2\Delta^2}[(\rho_{k+1}+\rho_k)f_{k+1} + (\rho_k + \rho_{k-1})f_{k-1} - (\rho_{k+1} + \rho_{k-1} + 2\rho_k)f_k],\end{aligned} \tag{B 6}$$

where $\rho_k = k\Delta$, $f_k = f(\rho_k)$ and $f'_k = f'(\rho_k)$. The above discretization allows us to preserve the vanishing boundary conditions on $\phi^{(n)}(\rho)$ at each step of the iteration. The functions $\phi^{(0)}(\rho)$ and

$\phi^{(n)}(\rho)$ in (B 4) are replaced with the N-dimensional arrays $\phi^{(0)}(\rho_k)$ and $\phi^{(n)}(\rho_k)$, $k=1,\ldots,N$, while the operators $\mathscr{M}$ and $\mathscr{L}$ with the $N\times N$ matrices $M_{ij}=\delta_{ij}m(\rho_i)/\rho_i$ and

$$\Lambda_{ij}=\delta_{ij}\frac{m(\rho_i)}{\rho_i}[U(\rho_i)-U_{\min}]+\frac{[\ln(1+\mu)]^2}{2\Delta^2}\times\begin{cases}(-\rho_{i-1}-\rho_i) & j=i-1\\ (\rho_{i-1}+2\rho_i+\rho_{i+1}) & j=i\\ (-\rho_i-\rho_{i+1}) & j=i+1\\ 0 & \text{otherwise,}\end{cases}\tag{B 7}$$

where $i,j=1,\ldots,N$ (no implicit sum on i). Likewise, the nth approximation to the lowest eigenvalue is calculated as follows:

$$\lambda_0^{(n)}\approx\frac{\sum_{i,j=1}^{N}\phi^{(n)}(\rho_i)\Lambda_{ij}\phi^{(n)}(\rho_j)}{\sum_{i,j=1}^{N}\phi^{(n)}(\rho_i)M_{ij}\phi^{(n)}(\rho_j)}.\tag{B 8}$$

To summarize, one starts from a trial array $\phi^{(0)}(\rho_k)$ satisfying the appropriate boundary conditions, repeatedly applies the matrix $\Lambda^{-1}M$ and calculates $\lambda_0^{(n)}$ from (B 8), until $|(\lambda_0^{(n)}-\lambda_0^{(n-1)})/\lambda_0^{(n)}|<\epsilon$ for a given ϵ. The array $\phi^{(n)}(\rho_k)$ is renormalized after every iteration.

The above procedure involves the parameters N, μ and ϵ. N and μ must be chosen in such a way as to accurately resolve $U_{\text{eff}}(\rho)$, namely the repulsive barrier at $\rho=1$, the potential well near to the diffusive scale, and the decay of the potential to zero at $\rho=0$. In particular, the choice of the values of N and μ requires some care for ξ near to 2, as the effective potential decays to zero slowly in that case. In our calculations, we varied N between 5×10^4 and 10^7 and μ between 10^{-5} and 5×10^{-2} according to the values of ξ and $\wp$. The threshold for the convergence, ϵ, needs to be sufficiently small, especially for ξ or $\wp$ close to 1, because the convergence to the theoretical eigenvalue may be rather slow for these values of ξ and $\wp$. In our calculations, ϵ was varied between 10^{-14} and 10^{-8}.

Appendix C. Structure functions for a finite Re_{m}

As mentioned in §1, the longitudinal and normal three-dimensional spectra of an isotropic random vector field (see [15, eqn. (12.31)] for the definitions) must be non-negative. When constructing the spatial correlation of such a field, it is therefore easier to first define the spectra according to the desired model and then derive the corresponding spatial correlations directly from these spectra.

Following [15], we thus introduce a finite Re_{m} in the Kazantsev model by assuming that the velocity spectrum has the form given in (3.20). Such a spectrum can be obtained by choosing the longitudinal and normal three-dimensional velocity spectra as follows:

$$F_{\text{L}}(k)=\wp\frac{A_{\text{P}}}{2\pi L^{\xi_{\text{P}}}}\frac{k^2}{(k^2+L^{-2})^{(5+\xi_{\text{P}})/2}}\tag{C 1}$$

and

$$F_{\text{N}}(k)=(1-\wp)\frac{A_{\text{S}}}{4\pi L^{\xi_{\text{S}}}}\frac{k^2}{(k^2+L^{-2})^{(5+\xi_{\text{S}})/2}}.\tag{C 2}$$

The structure functions corresponding to the above spectra are [15, p. 108]:

$$S_{\text{L}}(r)=(1-\wp)S_{\text{L}}^{(\text{S})}(r)+\wp S_{\text{L}}^{(\text{P})}(r)\tag{C 3}$$

and

$$S_{\text{N}}(r)=(1-\wp)S_{\text{N}}^{(\text{S})}(r)+\wp S_{\text{N}}^{(\text{P})}(r)\tag{C 4}$$

with

$$S_{\text{L}}^{(\text{S})}(r)=\frac{A_{\text{S}}\sqrt{\pi}}{4\Gamma((5+\xi_{\text{S}})/2)}\left[\Gamma\left(\frac{\xi_{\text{S}}}{2}\right)-2^{1-\xi_{\text{S}}/2}\left(\frac{r}{L}\right)^{\xi_{\text{S}}/2}K_{\xi_{\text{S}}/2}\left(\frac{r}{L}\right)\right]\tag{C 5}$$

and

$$S_{\mathrm{N}}^{(\mathrm{P})}(r) = \frac{A_{\mathrm{P}}\sqrt{\pi}}{4\Gamma((5+\xi_{\mathrm{P}})/2)}\left[\Gamma\left(\frac{\xi_{\mathrm{P}}}{2}\right) - 2^{1-\xi_{\mathrm{P}}/2}\left(\frac{r}{L}\right)^{\xi_{\mathrm{P}}/2} K_{\xi_{\mathrm{P}}/2}\left(\frac{r}{L}\right)\right], \tag{C 6}$$

$S_{\mathrm{N}}^{(\mathrm{S})}(r) = S_{\mathrm{L}}^{(\mathrm{S})}(r) + \frac{1}{2} r\, \mathrm{d}S_{\mathrm{L}}^{(\mathrm{S})}/\mathrm{d}r$ and $S_{\mathrm{L}}^{(\mathrm{P})}(r) = S_{\mathrm{N}}^{(\mathrm{P})}(r) + r\, \mathrm{d}S_{\mathrm{N}}^{(\mathrm{P})}/\mathrm{d}r$ (we remind the reader that our definition of the structure functions differ from that of [15] by a factor of 2).

For $r \ll L$, $S_{\mathrm{L}}(r)$ and $S_{\mathrm{N}}(r)$ reduce to the functions given in (3.15) and (3.16) with

$$D_{\mathrm{S}} = \frac{A_{\mathrm{S}}\Gamma(-1-\xi_{\mathrm{S}})}{(3+\xi_{\mathrm{S}})L^{\xi_{\mathrm{S}}}} \cos\frac{\pi\xi_{\mathrm{S}}}{2} \tag{C 7}$$

and

$$D_{\mathrm{P}} = \frac{A_{\mathrm{P}}\Gamma(-1-\xi_{\mathrm{P}})}{(3+\xi_{\mathrm{P}})L^{\xi_{\mathrm{P}}}} \cos\frac{\pi\xi_{\mathrm{P}}}{2}. \tag{C 8}$$

The structure functions for the case in which the solenoidal and potential parts of the velocity field have same scaling exponent can be derived from the above expressions by setting $\xi_{\mathrm{S}} = \xi_{\mathrm{P}} = \xi$ (see (2.5)).

References

1. Brandenburg A, Subramanian K. 2005 Astrophysical magnetic fields and nonlinear dynamo theory. *Phys. Rep.* **417**, 1–209. (doi:10.1016/j.physrep.2005.06.005)
2. Kazantsev AP. 1968 Enhancement of a magnetic field by a conducting fluid. *Sov. Phys. JETP* **26**, 1031.
3. Vergassola M. 1996 Anomalous scaling for passively advected magnetic fields. *Phys. Rev. E* **53**, R3021–R3024. (doi:10.1103/PhysRevE.53.R3021)
4. Kraichnan RH. 1968 Small-scale structure of a scalar field convected by turbulence. *Phys. Fluids* **11**, 945. (doi:10.1063/1.1692063)
5. Falkovich G, Gawędzki K, Vergassola M. 2001 Particles and fields in fluid turbulence. *Rev. Mod. Phys.* **73**, 913–975. (doi:10.1103/RevModPhys.73.913)
6. Federrath C, Chabrier G, Schober J, Banerjee R, Klessen RS, Schleicher DRG. 2011 Mach number dependence of turbulent magnetic field amplification: solenoidal versus compressive flows. *Phys. Rev. Lett.* **107**, 114504. (doi:10.1103/PhysRevLett.107.114504)
7. Federrath C, Schober J, Bovino S, Schleicher DRG. 2014 The turbulent dynamo in highly compressible supersonic plasmas. *Astrophys. J. Lett.* **797**, L19. (doi:10.1088/2041-8205/797/2/L19)
8. Federrath C. 2016 Magnetic field amplification in turbulent astrophysical plasmas. *J. Plasma Phys.* **82**, 535820601. (doi:10.1017/S0022377816001069)
9. Kazantsev AP, Ruzmaĭkin AA, Sokolov DD. 1985 Magnetic field transport in an acoustic turbulence type flow. *Sov. Phys. JETP* **88**, 487–494.
10. Rogachevskii I, Kleeorin N. 1997 Intermittency and anomalous scaling for magnetic fluctuations. *Phys. Rev. E* **56**, 417–426. (doi:10.1103/PhysRevE.56.417)
11. Schekochihin AA, Kulsrud RM. 2001 Finite-correlation-time effects in the kinematic dynamo problem. *Phys. Plasmas* **8**, 4937–4953. (doi:10.1063/1.1404383)
12. Schekochihin AA, Boldyrev SA, Kulsrud RM. 2002 Spectra and growth rates of fluctuating magnetic fields in the kinematic dynamo theory with large magnetic Prandtl numbers. *Astrophys. J.* **567**, 828–852. (doi:10.1086/apj.2002.567.issue-2)
13. Schober J, Schleicher D, Federrath C, Klessen R, Banerjee R. 2012 Magnetic field amplification by small-scale dynamo action: dependence on turbulence models and Reynolds and Prandtl numbers. *Phys. Rev. E* **85**, 026303. (doi:10.1103/PhysRevE.85.026303)
14. Subramanian K. 1997 Dynamics of fluctuating magnetic fields in turbulent dynamos incorporating ambipolar drifts. (http://arxiv.org/abs/astro-ph/9708216).
15. Monin AS, Yaglom AM. 1975 *Statistical fluid mechanics*, vol. II. Cambridge, MA: MIT Press.
16. Federrath C, Roman-Duval J, Klessen RS, Schmidt W, Mac Low M-M. 2010 Comparing the statistics of interstellar turbulence in simulations and observations: solenoidal versus compressive turbulence forcing. *Astron. Astrophys.* **512**, A81. (doi:10.1051/0004-6361/200912437)
17. Federrath C. 2013 On the universality of supersonic turbulence. *Mon. Not. R. Astron. Soc.* **436**, 1245–1257. (doi:10.1093/mnras/stt1644)

18. Wang J, Yang Y, Shi Y, Xiao Z, He XT, Chen S. 2013 Cascade of kinetic energy in three-dimensional compressible turbulence. *Phys. Rev. Lett.* **110**, 214505. (doi:10.1103/PhysRevLett.110.214505)
19. Wang J, Wan M, Song C, Xie C, Chen S. 2018 Effect of shock waves on the statistics and scaling in compressible isotropic turbulence. *Phys. Rev. E* **97**, 043108. (doi:10.1103/PhysRevE.97.043108)
20. Zeldovich YaB, Ruzmaikin AA, Sokoloff DD. 1990 *The almighty chance*. Singapore: World Scientific.
21. Tobias SM, Cattaneo F, Boldyrev S. 2012 MHD dynamos and turbulence. In *Ten chapters in turbulence* (eds P Davidson, Y Kaneda, KR Sreenivasan), p. 351. Cambridge, UK: Cambridge University Press.
22. Chandrasekhar S. 1961 *Hydrodynamic and hydromagnetic stability*. International Series of Monographs on Physics. Oxford, UK: Clarendon.
23. Robertson HP. 1940 The invariant theory of isotropic turbulence. *Proc. Camb. Phil. Soc.* **36**, 209–223. (doi:10.1017/S0305004100017199)
24. Frisch U. 1995 *Turbulence: the legacy of A.N. Kolmogorov*. Cambridge, UK: Cambridge University Press.
25. Elperin T, Kleeorin N, Rogachevskii I. 1995 Dynamics of the passive scalar in compressible turbulent flow: large-scale patterns and small-scale fluctuations. *Phys. Rev. E* **52**, 2617–2634. (doi:10.1103/PhysRevE.52.2617)
26. Celani A, Lanotte A, Mazzino A. 1999 Passive scalar intermittency in compressible flow. *Phys. Rev. E* **60**, R1138–R1141. (doi:10.1103/PhysRevE.60.R1138)
27. Gawędzki K, Vergassola M. 2000 Phase transition in the passive scalar advection. *Phys. D* **138**, 63–90. (doi:10.1016/S0167-2789(99)00171-2)
28. Zinn-Justin J. 1996 *Quantum field theory and critical phenomena*. Oxford, UK: Clarendon.
29. Mitra D, Brandenburg A. 2012 Scaling and intermittency in incoherent α-shear dynamo. *Mon. Not. R. Astron. Soc.* **420**, 2170–2177. (doi:10.1111/j.1365-2966.2011.20190.x)
30. Seshasayanan K, Alexakis A. 2016 Kazantsev model in non-helical 2.5-dimensional flows. *J. Fluid Mech.* **806**, 627–648. (doi:10.1017/jfm.2016.614)
31. Chertkov M, Falkovich G, Kolokolov I, Vergassola M. 1999 Small-scale turbulent dynamo. *Phys. Rev. Lett.* **83**, 4065–4068. (doi:10.1103/PhysRevLett.83.4065)
32. Landau LD, Lifshitz EM. 1958 *Quantum mechanics: non-relativistic theory*. New York, NY: Pergamon.
33. Gruzinov A, Cowley S, Sudan R. 1996 Small-scale-field dynamo. *Phys. Rev. Lett.* **77**, 4342–4345. (doi:10.1103/PhysRevLett.77.4342)
34. Vincenzi D. 2002 The Kraichnan-Kazantsev dynamo. *J. Stat. Phys.* **106**, 1073–1091. (doi:10.1023/A:1014089820881)
35. Arponen H, Horvai P. 2007 Dynamo effect in the Kraichnan magnetohydrodynamic turbulence. *J. Stat. Phys.* **129**, 205–239. (doi:10.1007/s10955-007-9399-5)
36. Zil'dovich IaB. 1957 The magnetic field in the two-dimensional motion of a conducting turbulent fluid. *J. Exp. Theor. Phys.* (*URSS*) **4**, 460.
37. Ruzmaĭkin AA, Sokolov DD. 1981 The magnetic field in mirror-invariant turbulence. *Sov. Astron. Lett.* **7**, 388–390.
38. Novikov VG, Ruzmaĭkin AA, Sokolov DD. 1983 Kinematic dynamo in a reflection-invariant random field. *Sov. Phys. JETP* **58**, 527.
39. Artamonova OB, Sokolov DD. 1986 Asymptotic study of the rapid growth of the second moment of a magnetic field in mirror-symmetric flow. *Vestn. Moscow Univ., Ser. III, Fiz. Astronom.* **27**, 8–13.
40. Maslova TB, Ruzmaikin AA. 1987 Growth of magnetic field fluctuations in a turbulent flow. *Magnitnaia Gidrodinamika* **23**, 3–7.
41. Ruzmaikin A, Sokoloff D, Shukurov A. 1989 The dynamo origin of magnetic fields in galaxy clusters. *Mon. Not. R. Astron. Soc.* **241**, 1–14. (doi:10.1093/mnras/241.1.1)
42. Seshasayanan K, Pétrélis F. 2018 Growth rate distribution and intermittency in kinematic turbulent dynamos: which moment predicts the dynamo onset? *Europhys. Lett.* **122**, 64004. (doi:10.1209/0295-5075/122/64004)
43. Morse PM, Feshbach H. 1953 *Methods of theoretical physics*, vol. I. New York, NY: McGraw-Hill.